
Article:
Postulkova, H., Nedomova, E., Hearnden, V. orcid.org/0000-0003-0838-7783 et al. (2 more authors) (2019) Hybrid hydrogels based on polysaccharide gum karaya, poly(vinyl alcohol) and silk fibroin. Materials Research Express, 6 (3). 035304. ISSN 2053-1591

https://doi.org/10.1088/2053-1591/aaf45d

Hybrid hydrogels based on polysaccharide gum karaya, poly(vinyl alcohol) and silk fibroin

Received xxxxxx
Accepted for publication xxxxxx
Published xxxxxx

Abstract

This work focuses on preparation of a hybrid hydrogel consisting of both natural and synthetic polymers including the polysaccharide gum karaya which is both inexpensive and abundant, the protein silk fibroin which exhibits remarkable mechanical properties and poly(vinyl alcohol). These polymers were primarily selected due to their biocompatibility, but also through their ability to be combined together in an aqueous, non-toxic route, thus facilitating their potential future use as burn dressings. A range of structural, mechanical and practical techniques were employed to characterise the hydrogels including, FTIR, UV/VIS, phase contrast microscopy, XRD, DMA, swelling and hydrolytic stability. Finally, looking towards application as a dressing, these materials demonstrated low cell adhesion through a keratinocyte cell culture assay. The results support both the potential application of these hydrogels and provide insight into the role of each component polymer in the material. Therefore, we propose hybrid hydrogels such as these offer a unique combination of performance, ease of processing and low cost that can serve as inspiration for the next wave of bespoke medical products.

Keywords: Biocompatible polymers; Hydrogel; Gum Karaya; Poly(vinyl alcohol); Silk fibroin

1. Introduction

Gels are cross-linked macromolecular networks swollen in a liquid [1–3] and if done so in water are termed hydrogels [4]. Their three-dimensional networks are capable of retaining large volumes of water or biological fluids (up to thousands of times their dry weight) [5]. As such hydrogels are widely studied in biomedical applications because their physical properties are similar to human tissues and they possess excellent biocompatibility [6] making them highly desirable for burns treatment.

Specifically for burns treatment, hydrogels provide a moist environment which is has been shown to be an important factor in accelerating the wound healing process [7] as well as providing a cooling effect, a barrier against infection and can be easily removed without pain [3,7–10]. Yet despite several solutions currently on the market there is still plenty of room for improvement and designing hydrogels and skin wound coverings that satisfy a range of technical requirements, at an affordable price, is a big challenge [11–14]. However, previous work has suggested a potential solution; a hybrid hydrogel material based on a mixture of natural and synthetic biopolymers which can meet these complex requirements for successful wound healing [15].

Addressing this challenge, this work focuses on the combination of four types of biomaterials in order to design hydrogels for potential future use in burns treatment. These hydrogels are based on a natural polysaccharide, gum karaya, a natural protein, silk fibroin, a synthetic biopolymer poly(vinyl alcohol) and finally glycerol.

Gum karaya (Sterculia urens, GK) is a natural gum which consists of a complex, branched and partially acetylated, hydrophilic, anionic polysaccharide containing β-D-galactose, L-rhamnose, β-D-glucuronic acid and D-galacturonic acid. It is commonly available and is considered

a relatively cheap, biodegradable and biocompatible material [9,16]. GK has garnered widspread interest as it has unique material features such as a high viscosity and capacity for swelling and water retention, it is both gel and film forming and has adhesive properties [16]. From a chemical perspective GK is resistant to hydrolysis by mild acid and is partly resistant to bacterial and enzymatic degradation [16,17]. In recent years, GK and its combination with other polymers has been explored when developing hydrogels for drug delivery systems (i.e. with PVA [3,8,9,18], acrylic acid [19,20] and others [2,17,20,21]). However its potential has been somewhat limited due to its water solubility, although this can be altered through alkali treatment [22].

Poly(vinyl alcohol) (PVA) is a biocompatible, hydrophilic water soluble polymer [8,18,23] which is not biodegradable in most physiological conditions [24]. It is widely used in biomedical and tissue engineering applications because of its good processability, ability to form films, mechanical properties (e.g. sufficient strength) and temperature stability [8,25]. Hydrogels based on PVA are mainly prepared by crosslinking (e.g. glutaraldehyde) [26] or radiation and repeated freezing/thawing methods [24,27]

PVA has been previously combined with different types of biopolymers to obtain hydrogels for tissue engineering, for example with chitosan [25], starch [28], cellulose [6], alginate [29], dextran, glucan [30], gelatine [31], PVP [32], silk fibroin [33] etc. Hydrogels based on PVA and polysaccharides have been found to be suitable for producing transparent, flexible, mechanically strong, biocompatible, effective and economical hydrogel dressings [3,20]. PVA is also known as a anti-biofouling material i.e. it is a non-favourable substrate for cell adhesion, proliferation and exhibits minimal adsorption of proteins [23]. Such a combination of desirable properties makes PVA an excellent candidate for the use in burn dressings because of the need for frequent dressing changes on wounds without destroying newly grown tissue underneath.

Over the past decade silk fibroin (SF) has rapidly become a biomaterial of choice for a range of applications due to a combination of excellent intrinsic mechanical properties, biocompatibility, biodegradability [34,35] and extrinsic properties achieved through aqueous processing such as film formation, oxygen permeability and ease of sterilisation [34,36–38]. Extending its capability, silk has been used in mixtures with other biomaterials to create films or hydrogels for biomedical applications including alginate [39], hyaluronic acid [40], chitosan [41], PVA [42–44], PEG [45], polyacrylamide [46] and polyurethane [47].

Finally glycerol is a non-toxic, low molecular weight compound which is also often used in biomedical applications as a plasticizer [38]. This is best evidenced in the case of PVA/SF hydrogel blends where glycerol has been used to improve mechanical properties for over a decade [48] and has been shown to reduce the degree of phase separation, acting as a compatibiliser and resulting in increased breaking strength and elongation of films [38].

Therefore, under the premise that a combination of the above materials can be determined that results in a hybrid hydrogel whose properties exceed that of any individual materials contribution. This work reports the preparation of hydrogels based on natural polysaccharide gum karaya, synthetic biopolymer poly(vinyl alcohol) and protein silk fibroin and subject them to characterisation by FTIR, UV/VIS, phase contrast microscopy, XRD, DMA, swelling and stability studies and cell culture assays.

2. Materials and methods

2.1 Chemicals

Gum karaya was purchased from Sigma-Aldrich (M_w of approx. 9 500 000 $g \cdot mol^{-1}$), sodium hydroxide and hydrochloric acid were purchased from Lach-Ner, s.r.o., Czech Republic, ethanol (96%) was obtained from Moravian distillery of Kojetín, Czech Republic, ultrapure water (Type I, resistivity 18.2 MΩ·cm) was prepared by a MilliQ Plus 185 machine and distilled water (Type II, resistivity 15 MΩ·cm) was prepared by a Bibby Merit 4000 still. Lithium bromide, sodium carbonate, poly(vinyl alcohol) (M_w 130 000, 99+% hydrolysed) were purchased from Sigma-Aldrich and glycerol (99 wt. %) from Fisher Scientific. Silkworm cocoons (commercial grade) were spun in-house from a stock of B. mori silkworms. Dulbecco's medium, fetal calf serum, L-Glutamine, penicillin, MTT solution and resazurin solution was purchased from (Sigma Aldrich, Dorset, UK).

2.2 Chemicals Solubilisation and purification of raw gum karaya

Raw gum karaya powder was combined with ultrapure water and magnetically stirred at 300 rpm in a beaker for 24 hours at room temperature to obtain a visually homogenous dispersion. Solubilisation was carried out following a previously described deacetylation method [49]. Briefly, a dispersion of GK was solubilized by sodium hydroxide (1 mol/l). Three volumes of a GK dispersion were mixed with one volume of hydroxide solution and stirred for 5 minutes at room temperature. Diluted hydrochloric acid was used to neutralize any excess hydroxide after GK solubilisation. The solubilized sample of GK was filtered through polypropylene filters (pore size of 42 μm) and centrifuged for 40 minutes at 40 °C, 15 000 rpm to remove impurities. Afterwards the samples were filtered again through a paper filter (pore size 4–7 μm). The sample was then precipitated with ethanol in a ratio 2:1 and air-dried for

24 hours. Finally the dry sample was powdered and stored in a glass vial.

2.3 Degumming process of silk fibroin (SF)

Commercial quality B. mori silkworm cocoons were cut into small pieces (~4 mm^2) and washed with distilled water in a food processor at its highest speed for 15 minutes three times. They were washed again with sodium carbonate solution having 0.05 mol/l concentration (70 °C) using the food processor for 20 minutes four times and finally washed with distilled water. Fibres were dried in an oven at 50 °C overnight. Finally, dry fibres were blended in the food processor for 5 minutes to become 'fluffy' to assist with the following dissolution.

2.4 Dissolution of silk

Dissolution of silk fibres was carried out with 9.3 mol/l lithium bromide at 70 °C in a water bath for 80 minutes. The resulting solution was dialysed in a dialysis bag (molecular weight cut-off 12-14 000 $g \cdot mol^{-1}$) against ultrapure Type I water for 2 days at 4 °C and then stored in the fridge until required. The concentration of silk solution was determined by gravimetry and then diluted to 1 wt. % solution with ultrapure water.

2.5 Preparation of hydrogels based on blend of gum karaya, poly (vinyl alcohol), silk fibroin and glycerol

GK and PVA were dissolved together in ultrapure Type I water to prepare 0.3 wt. % and 3 wt. % solutions, respectively. GK/PVA solution was prepared by dissolving raw powders of GK and PVA together to produce final concentration of GK 0.3 wt. % and PVA 3 wt. % in a given volume. The solution was made by dissolving polymers overnight on hot plate stirrer at 90 °C. The solution was then dialysed against ultrapure Type I water for 2 days at 4 °C (molecular weight cut-off 12-14 000 $g \cdot mol^{-1}$) and then filtered through filter paper. GK/PVA solution was mixed in 2 ml Eppendorf tubes with different ratios of 1 wt.% silk solution and glycerol (G). Ratios of solutions used for hydrogel mixtures are described in Table 1. Solutions were mixed overnight at room temperature and then cast onto round 35 mm Petri dishes and dried on an orbital shaker in a fume hood. The resulting dry Xerogels (in a film form) were peeled off the next day and stored in plastic bags.

2.6 Characterisation

2.6.1 Attenuated Total Reflectance - Fourier Transform Infrared Spectroscopy

Infrared spectra were recorded with a NICOLET 380 FTIR spectrometer (Thermo Scientific) purged with dry air between 4 000 and 800 cm^{-1} averaging 32 scans and a

resolution of 4 cm^{-1} The samples were analysed in xerogel form using an attenuated total reflection (ATR) accessory with a diamond crystal (Golden Gate, Specac, UK).

2.6.2 Ultraviolet–Visible Spectroscopy

UV/VIS analysis was carried out with UV2 UV/VIS Spectrometer (UNICAM). Spectra were recorded between 200 and 800 nm with lamp change was at 340 nm applying 240 $nm.min^{-1}$ speed with 2 nm data point intervals.

2.6.3 Phase Contrast Microscopy

Phase contrast microscopy was carried out using an inverted Nikon Diaphot microscope (Nikon systems, Japan) and phase contrast optics with 10, 20 and 40x objectives and imaged using a Motic Moticam 5MP digital camera (Motic Systems, Spain).

2.6.4 X-ray diffraction (XRD)

X-ray diffraction analysis was carried out on a benchtop X-ray diffractometer Rigaku MiniFlex 600 using Cu anode, 40 kV tube voltage and 15 mA tube current. Xerogel films (2x2 cm) were analysed in scanning range from 2 to 60° (2θ).

2.6.5 Dynamical Mechanical Analysis (DMA)

DMA measurements were performed using a TA Instruments DMA Q800 Dynamic Mechanical Analyser (TA Instruments, Delaware, USA) equipped with the film/fibre tension accessory. Xerogel films were heated under a nitrogen atmosphere from -100 to 220 °C at a heating rate of 3 °C/min with frequency of 1 Hz, 0.01% strain and 1N preload.

2.6.6 Swelling behaviour

Hydrogel swelling was carried out in Type I water using the gravimetric method. Xerogel films were cut into small pieces of the same weight (approximately 1x1 cm), put onto Petri's dishes and immersed in an excess of ultrapure Type 1 water. At set time points (1, 3, 5, 7, 10, 20, 30, 40, 60 and 120 minutes), the excess water in the Petri dish was removed by paper tissue and the hydrogel was immediately weighed. The swelling ratio was calculated as

$$Swelling\ ratio = \left(\frac{W_s - W_d}{W_d}\right) \quad (1)$$

where W_s is weight of swollen hydrogel and W_d is weight of xerogel.

2.6.7 Hydrogel stability

After swelling, a stability test was carried out. Samples were placed into vials and immersed in ultrapure Type I and kept in an incubator at 37 °C. Resulting hydrogel stability was measured on day 3, 10, 20 and 60. To do so, samples were removed from their vials and weighed to determine the weight loss. Hydrogel stability was calculated using the formula (2), where w_t is the weight of sample at a specific timepoint and w_0 is the dry weight of initial mass of sample.

$$Hydrogel\ stability = \left(\frac{w_t}{w_0}\right) \times w_0 \quad (2)$$

2.6.8 Adhesion test and MTT proliferation assay

A HaCaT skin keratinocyte cell line was used and cells grown in cell culture media consisting of Dulbecco's Modified Eagle's medium (DMEM) supplemented with 10% (v/v) fetal calf serum, 100i.u./ml penicillin and 100µg/ml streptomycin and 2mmol/l L-Glutamine (Sigma Aldrich) and cultured in a humidified cell culture incubator at 37°C with 5% CO_2. Xerogels were sterilised using UV light (emission 253.7 nm) in Esco Labculture Class II Biological Safety Cabinet for 40 min.

The adhesion assay was performed with HaCaT keratinocyte cell line cultured in 6 well plates. A confluent layer of HaCaT cells (cell number ~400 000) was seeded onto the tissue culture plastic surface of the 6 well plate to produce a layer of epithelium. Sterilised hydrogel discs (1 cm in diameter) were then added into wells and left to swell in cell culture media for 30 min. After 30 minutes, hydrogel discs were weighed down by light metal grid to ensure contact between the hydrogel and the cell layer. After 24 hours of direct contact, hydrogels were peeled off the cell layer and both the hydrogel surface and cell layer were examined with using phase contrast light microscopy for signs of cell adhesion.

An MTT (3-(4,5- dimethylthiazol-2-yl)-2, 5-diphenyltetrazolium bromide) assay was used to measure cell adhesion and survival on the tissue culture plastic (TCP) surface and on hydrogel surfaces. 2 ml of 0.5 mg/ml MTT solution (Sigma Aldrich) in PBS was added to cells or hydrogels and incubated for 40 min. After 40 minutes, the unreacted MTT solution was removed and the purple intracellular formazan salt (produced by dehydrogenase reduction of MTT) was solubilised and released from cells using acidified isopropanol (125µl of 10 mol/l HCl in 100ml isopropanol). The eluted dye was transferred to a 96 well plate. The optical density of the solution was measured at 540nm with a reference at 630nm, using a spectrophotometer (BioTek ELx800). A positive control was conducted which represents results from cells which were not in contact with a hydrogel and the negative control represents measurements from wells without any cells present.

3. Results and discussion

Transparent and flexible hydrogels were prepared by physical crosslinking based on strong intra and intermolecular hydrogen bonds in PVA with a high degree of

hydrolysis [23]. Not using a chemical crosslinker was desirable as this lowers the possibility of negative effects of unreacted crosslinker on cell viability and thus the overall healing process, simplifies regulatory approval as well as reducing the overall cost of production. We estimate the price of 1 cm^2 of prepared hydrogel in this study to be ~£0.02/$0.03 (based on material costs for 10cm^2 of a ~40 µm thick hydrogel). In comparison, complex dermal treatment applications as Integra (silicone layer on top of a porous matrix comprising a chemically cross-linked coprecipitate of bovine collagen and shark-derived chondroitin-6-sulfate) costs about $15–30 per cm^2 [12]. Subsequently the prepared xerogels were characterized by various techniques to understand their properties, structure and mutual interaction of the materials when combined together.

3.1 Effect of composition on chemical structure

FTIR spectroscopy was used to characterize specific chemical groups in the individual materials which can then be used to inform of their presence or absence in subsequent blends. Individually, spectra of GK, PVA, SF and final blended xerogel films are depicted in

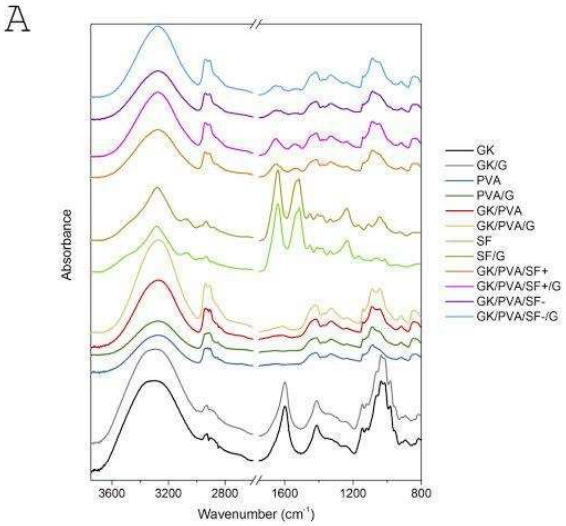

Figure 1A. The ATR-FTIR spectra of GK shows a diagnostic broad peak of hydroxyl stretching at 3650-3000 cm^{-1} [9], stretching of aliphatic C-H bonds at 2920 cm^{-1} [9], vibrations of carboxylate salt group (-COO-) at 1605 and 1418 cm^{-1} [50] and C-O stretching and group vibration of sugar rings at 1180–940 cm^{-1} [51]. For PVA spectra the band for CH2 groups at 1470-1410 cm^{-1} [52], resonance of CH-OH at 1320 cm^{-1} [53] and broad band representing C-O bonds at 1150-1085 [52] are indicative of its presence. Significant bands in SF spectra represent the OH and NH stretching at 3600-3100 cm^{-1}, amide I, II and III at 1640, 1510 and 1230 cm^{-1}, respectively. The peak at 1050 cm^{-1} belongs to vibration of serine [54].

When investigating subsequent blends to confirm all introduced materials are present, spectra of a GK/PVA mixture clearly shows a combination of characteristic bands for PVA and GK. However in these spectra bands assigned to GK were less distinctive which we believe is due to its lower ratio in the mixture. Hence bands are not only a useful indicator of presence, but band intensity also informs of a materials' relative proportion in the xero/hydrogels.

Spectra of the xerogel films most suited towards potential application and explored via cell culture later, contain primarily bands of PVA and SF which are the major components of these samples. As can be seen from the spectra in Figure 1, GK/PVA/SF- and GK/PVA/SF-/G spectra show a decreased intensity in bands related to amide I and II due to lower SF ratio compared to GK/PVA/SF+ and GK/PVA/SF+/G.

Finally the addition of glycerol increased the intensity of the broad peak representing hydroxyl stretching (3650-3000 cm^{-1}) for samples GK/PVA/G, GK/PVA/SF+/G and GK/PVA/SF-/G due to presence of hydroxyl groups in glycerol structure [48].

The UV/VIS absorption spectra of prepared xerogel films are shown in

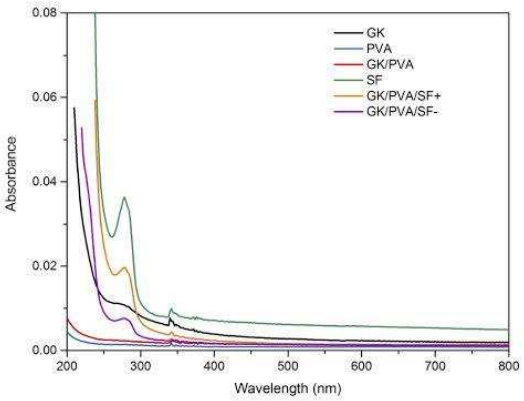

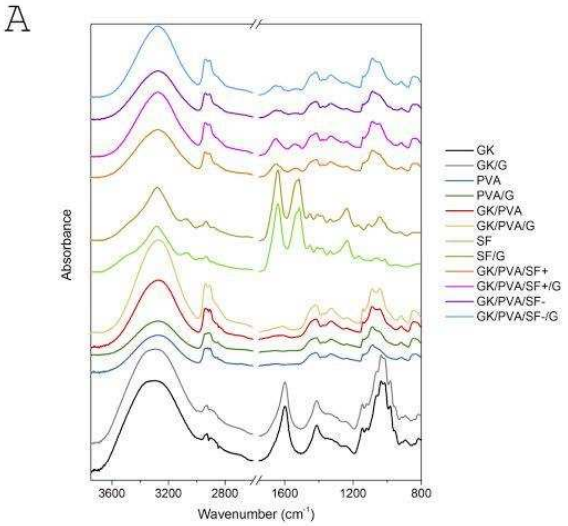

Figure 1B. Absorption spectra of samples containing silk fibroin displayed a wide peak in region of 250-300 nm. The main chromophores absorbing in this region are aromatic amino acids such as tyrosine and tryptophan which are known to be present in silk [55]. The absorbance observed in these samples is further confirmed to be attributed to silk as the intensity of UV absorption for tyrosine peak decreases with decreasing silk content of the samples (SF>GK/PVA/SF+>GK/PVA/SF-).

A minor increase in absorbance was observed for GK samples in the same region as for silk whereas samples where PVA was major component (PVA and GK/PVA samples) did not show any UV absorbance. This increase in absorption at the beginning of the spectra is therefore most probably caused by water adsorbing to the dried xerogel films [56], which speak to the ability of GK to become hydrated easily. All samples had a very low absorbance in the rest of the spectra towards higher wavelengths and notably the addition of glycerol did not affect the UV/VIS spectra of any of the films. These results are important as it clearly demonstrates a high degree of transmission/transparency in the visible range of light. This is particularly useful for wound dressings as it would enable the underlying tissues to be inspected by healthcare professionals without the need to remove the dressing.

3.2 Morphology of xerogel film surfaces

Phase contrast microscopy was carried out to characterize the morphology of xerogel film surfaces and study any potential macroscale phase separation of the materials in the films (Figure 2). GK and GK/G films were smooth with only small aggregates or bubbles (Figure 2A, B). Films from PVA and GK/PVA (Figure 2C, E) were also smooth, lacking any significant surface morphology. However SF films displayed both surface roughness and inhomogeneities (Figure 2G). Looking towards the blends, the GK/PVA/SF+ sample (Figure 2I) had a similar structure to SF. This structure is not homogenous and indicative of a phase separation which appears to happen spontaneously when SF and PVA solution are mixed together and cast into films [57]. GK/PVA/SF- (Figure 2K) also showed phase separation but in this case, a finer dispersion was observed with smaller particles due to the lower SF content. Previosuly it has been shown that particle size in PVA/SF system with phase separation can be tailored by sonication [57] and this may be a useful strategy to adopt in future studies. Finally it was seen that addition of glycerol to the films did not have any noticeable effect on hydrogel morphology and phase distribution.

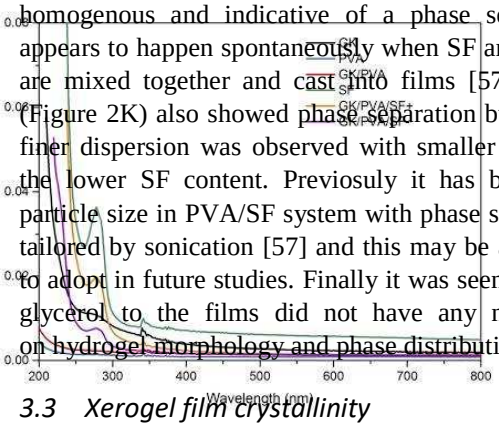

3.3 Xerogel film crystallinity

XRD measurements were used to evaluate the crystallinity of the separate raw materials and prepared blended xerogel films. GK and all SF samples clearly showed an amorphous structure. This is not particularly surprising as GK is a branched polysaccharide with non-repetitive structures and thus an amorphous nature was expected. In contrast, SF has ability to form ordered structures including β-sheets [36], however the ability of SF molecules to create these more crystalline structures can be lost due to the detrimental effects of the preparation/reconstitution process [58].

PVA also has crystalline and regular regions in its structure, but their extent is determined by the level of PVA hydrolysis [26]. In our measurements, pellets of PVA showed a characteristic peak for PVA at 20° (Figure 3) which is the main crystal peak, corresponding to a (101) reflection of the monoclinic crystal [59]. Subsequent lower peak intensities and therefore less developed crystalline structures (i.e. minor peaks not present) was observed for the PVA film and all samples with PVA content. This could be a result of the preparation method, as solutions were dried whilst being gently mixed. This drying method could disturb the development of the crystalline structure of a PVA xerogel film compared to that observed in PVA pellets. Formation of PVA crystalline and regular regions could be also affected by the presence of other types of polymers in system whose chains could restrict the ability of the PVA polymer chains to crystalise. Following on from this, an effect of SF content towards hydrogel crystallinity was observed. Samples containing a higher ratio of SF (GK/PVA/SF+ and GK/PVA/SF+/G) showed lower crystallinity; this could be caused generally by a lower ratio of PVA in system but also by the higher SF content which contributes more towards restriction of PVA crystalline regions formation.

Interestingly, the addition of glycerol clearly affected xerogel film crystallinity. Samples with glycerol tended to show a higher intensity peak on XRD. This could suggest that as glycerol acts as a plasticiser is essentially increases free

volume and supports movement/reptation of polymer chains, promoting higher sample crystallinity. However, this influence was not significant for PVA/G and SF samples.

3.4 The effect of structure on the xerogel film viscoelasticity

Dynamical mechanical analysis (DMA) was conducted to measure changes in viscoelasticity of xerogel films in dry state as a result of structural relaxation changes.

Xerogels based only on GK or SF could not be tested because of their brittle nature. All samples containing PVA showed the same general trend during testing (exemplar data depicted in (Figure 4A). From these DMA traces the storage modulus is related to a material's ability to store energy and its stiffness. A steady decrease in the storage modulus is observed from the beginning of the test, as temperature increased from -100 to 20 °C and is related to the softening of the material as a result of gamma and beta transitions (i.e. the beginning of localized bond movements and bending, stretching and side chain movements). The broad band for the loss modulus at the beginning of the test shows energy dissipation.

Following, the xerogel films show a significant decrease in storage modulus (approx. at 50 °C) and concurrent maximum in loss modulus which is related to the glass transition (Tg) of major component (PVA). This Tg is more easily denoted by investigating the tan delta signal for a peak (Figure 4B) which is reached slightly after maximum of loss modulus (which is indicative of a second-order phase transition). It is also worth noting that the Tg for the sample GK/PVA/SF-/G is slightly reduced by presence of glycerol because of its plasticising character.

Loss modulus showed another softening band in the 90-110 °C region which could be potentially related to structure reordering (possibly reordering amorphous PVA structures into crystalline ones). This transition is significantly affected by glycerol which reduces the temperature of this effect, lowering its intensity and somehow merging this transition together with band for the Tg (Figure 4A). Interestingly, a slight increase of storage modulus (intepretted as a hardening of the material) has been also observed in the region (above 100 °C) for both samples.

The aforementioned effect of glycerol on xerogel film properties is also apparent from tan delta plot (Figure 4B). Glycerol serves to merge peaks together, broadening them and suggesting its positive effect on mixing and blending the polymeric components present, thus also acting as a compatibilser. Here glycerol probably promotes and increases interactions between different types of polymer chains due to hydrogen bonding of hydroxyl groups of GK, PVA and glycerol and amide groups of SF [48,60].

The glass transition temperature of SF is not apparent in loss modulus data due to its low content in the film. However, the ordered structures Tg of SF can be observed in the tan delta signal as it usually appears at ~210 °C for B. mori silk [61] Figure 4B. This transition is clearly present for samples with higher SF content but is barely visible from samples with a low SF content. Interestingly, the temperature for SF's Tgin the GK/PVA/SF+/G blend is significantly affected by the presence of glycerol, reducing the transition temperature to around 160 °C which would be indicative of promoting more disordered structures in the film.

3.5 Swelling behaviour

The effect of various materials and their ratios on hydrogel water absorption (swelling) were carried out. Pure GK and SF samples were immediately water soluble, thus their swelling properties were not studied.

The highest swelling ratio (above 25x) was observed in samples with GK (GK/PVA and GK/PVA/G). Despite the low amount of GK present in the samples, the hydrogel showed the highest swelling potential (Figure 5A). However, any significant effect of glycerol on hydrogel swelling was not observed. The glycerol physical crosslinking clearly had a greater influence on the hydrolytic stability of hydrogels as discussed below.

The remaining samples showed similar and relatively stable swelling profiles (around 15x) which remained consistent through the 2 hours of the test. At the end of the test all samples had stabilised their swelling ratio apart to GK/PVA/SF+ which showed a lower swelling ratio throughout the whole test. These observations are in agreement with work studying PVA/SF hydrogels and their water uptake [62]. No significant difference was observed in the swelling regardless amount of added silk. This supports a hypothesis that the higher swelling in samples GK/PVA and GK/PVA/G is caused by the presence of GK.

3.6 Hydrogel stability

A study focused on hydrogel stability was carried out to evaluate stability in ultrapure Type I water at 37 °C over a 60 day period. Hydrogel stability is depicted in Figure 5B. the results indicate that hydrogel stability is largely based on the ability of PVA to form a physically crosslinked structure connected by hydrogen bonds [63] without any chemical crosslinking and the structure present is stable over a long time period.

Samples with different SF ratios (although otherwise with the same composition) have similar stabilities, suggesting that SF content did not have any significant effect towards hydrogel stability. Improvements in stability of PVA/SF cryo-hydrogels has been previously reported whereby a freeze-thaw regime for cryogels fabrication which ensured better stability in PBS at 37 °C[62].

The presenence of glycerol improved hydrogel stability was observed for all samples. This is most likely due to the

compatbilising action of glycerol as previously discussed, for our results are in good agreement with observations from DMA and XRD testing (see above) and previous observations on stability in SF hydrogels [38].

3.7 Adhesion test and MTT proliferation assay

A specific assay was developed to study adhesion of prepared hydrogels to a keratinocyte cell layer in order to to simulate a real-world scenario where a hydrogel dressing would be placed onto the skin surface. In this assay hydrogels were in contact with a confluent layer of keratinocytes for 24 hours prior to being removed and cell attachment measured.

As a broad observation, all hydrogels did not show any adhesion to the cell layer after weight removal and they were freely floating in the culture medium. Furthermore, using microscopy, no cells were observed on hydrogel surfaces of PVA, PVA/G, GK/PVA and GK/PVA/G (Figure 6 A-D) which suggests a low preference of keratinocytes to adhere to the hydrogel. However, the presence of keratinocytes on samples containing SF (Figure 6 E-H) could not be determined by imaging alone because the inherent microstructure of these materials when imaged using phase contrast microscopy gave an uneven appearance.

Therefore, moving past a qualitative visual analysis, in order to quantify cell attachment to the hydrogels an MTT assay was conducted. In addition, an MTT was performed on the confluent layer of cells on the tissue culture plastic to determine if contact with the hydrogel resulted in cell detachment or a reduction in cell viability (either through direct contact with the material or through contact with gel components eluted during swelling and incubation).

The MTT assay was unable to detect any metabolic activity from cells on the hydrogel surface, demonstrating no viable cells adhered to the material. This low adherence of cells on the hydrogel surface is most likely caused by the high content of PVA which is recognised as a non-favourable substrate for cell adhesion and proliferation [23]. However this is ideal for these films' potential application, as low adhesion of a hydrogel towards cells is essential for a wound dressing to avoid removal of any regenerating epithelium when the dressing is applied and subsequently replaced.

Figure 7 shows the metabolic activity of HaCaT cells following contact with each type of hydrogel. The positive control (cells without any hydrogel contact) demonstrated the highest cell activity while all wells with hydrogel contact displayed a slightly reduced cell metabolic activity compared to the positive control. This is likely as a result of the mechanical disruption as a result of the direct contact assay performed. The highest viability was observed in the samples containing SF. This observation is in agreement with [34,64] where SF has been described as supporting and promoting keratinocyte cells.

This data demonstrates that contact with hydrogels largely maintains cell viability. There is no evidence that the hydrogels are able to promote cell proliferation in this short term, two-dimensional cell culture assay. Here further studies are required to determine if the hydrogels are able to promote reepithelialisation in a wound healing model and to fully examine the effect of the material on skin cell viability and integrity.

4. Conclusion

Novel hydrogels based on a natural polysaccharide gum karaya, the synthetic biopolymer poly (vinyl alcohol) and the protein silk fibroin, were designed to address the challenge of developing suitable wound coverings . A range of hydrogels were produced and studied using different techniques such as FTIR, UV/VIS, phase contrast microscopy, XRD, DMA, swelling and stability studies as well as cell culture assays. The results have helped us to better to understand the structure, interactions and function of the constituent materials and their contributions towards the final extrinsic properties of hydrogels. From the results we propose that hydrogel stability in water is based on PVA's ability to create a partly crystalline structure which acts as physical crosslinking. Furthermore, DMA and stability studies showed a significant positive effect of glycerol towards improving hydrogel properties. Finally, cell culture showed that the hydrogels produced were non-toxic towards keratinocytes and they exhibited a low adhesion to them. Low cell adhesion is an essential feature for hydrogels to be successfully used for burnt skin regeneration to prevent destroying newly grown tissue as the covering is replaced. We conclude that the presented method of hydrogel preparation is straightforward, non-expensive and does not use any toxic chemicals. Therefore this study seeks to increase the potential of these materials to further develop new types of affordable and widely available biomedical materials; hybrid hydrogels for skin burn treatment.

Acknowledgements

References

[1] TEOH, S.H. and ACHAUER, B.M. (2004) Engineering materials for biomedical applications. 2nd ed. Hong Kong: World Scientific Pub.

[2] Singh, B. and Sharma, N. (2008) Modification of sterculia gum with methacrylic acid to prepare a novel drug delivery system. International Journal of Biological Macromolecules, **43**, 142–50. https://doi.org/10.1016/j.ijbiomac.2008.04.008

[3] Singh, B. and Pal, L. (2008) Development of sterculia gum based wound dressings for use in drug delivery. European Polymer Journal, **44**, 3222–30. https://doi.org/10.1016/j.eurpolymj.2008.07.013

[4] HU, J. and ACHAUER, B.M. (2011) Adaptive and functional polymers, textiles and their applications: an introduction to materials in medicine. 2nd ed. Hackensack, N.J.: Distributed by World Scientific, Pub. Co. Pte. Ltd.

[5] Hoffman, A.S. (2012) Hydrogels for biomedical applications. Adv. Drug Deliv. Rev. p. 18–23. https://doi.org/10.1016/j.addr.2012.09.010

[6] Chang, C., Lue, A. and Zhang, L. (2008) Effects of crosslinking methods on structure and properties of cellulose/PVA hydrogels. Macromolecular Chemistry and Physics, **209**, 1266–73. https://doi.org/10.1002/macp.200800161

[7] Caló, E. and Khutoryanskiy, V. V. (2015) Biomedical applications of hydrogels: a review of patents and commercial products. European Polymer Journal, **65**, 252–67. https://doi.org/10.1016/j.eurpolymj.2014.11.024

[8] Singh, B. and Pal, L. (2011) Radiation crosslinking polymerization of sterculia polysaccharide–PVA–PVP for making hydrogel wound dressings. International Journal of Biological Macromolecules, **48**, 501–10. https://doi.org/10.1016/j.ijbiomac.2011.01.013

[9] Singh, B. and Pal, L. (2012) Sterculia crosslinked PVA and PVA-poly(AAm) hydrogel wound dressings for slow drug delivery: Mechanical, mucoadhesive, biocompatible and permeability properties. Journal of the Mechanical Behavior of Biomedical Materials, Elsevier Ltd. **9**, 9–21. https://doi.org/10.1016/j.jmbbm.2012.01.021

[10] Kujath, P. and Michelsen, A. (2008) Wounds - from physiology to wound dressing. Deutsches Ärzteblatt International, **105**, 239–48. https://doi.org/10.3238/arztebl.2008.0239

[11] Selig, H.F., Lumenta, D.B., Giretzlehner, M., Jeschke, M.G., Upton, D. and Kamolz, L.P. (2012) The properties of an "ideal" burn wound dressing--what do we need in daily clinical practice? Results of a worldwide online survey among burn care specialists. Burns, Elsevier. **38**, 960–6. https://doi.org/10.1016/j.burns.2012.04.007

[12] Debels, H., Hamdi, M., Abberton, K. and Morrison, W. (2015) Dermal matrices and bioengineered skin substitutes: a critical review of current options. Plastic and Reconstructive Surgery Global Open, **3**, e284. https://doi.org/10.1097/GOX.0000000000000219

[13] Boateng, J. and Catanzano, O. (2015) Advanced Therapeutic Dressings for Effective Wound Healing—A Review. Journal of Pharmaceutical Sciences, Elsevier. **104**, 3653–80. https://doi.org/10.1002/JPS.24610

[14] Kamoun, E.A., Kenawy, E.R.S. and Chen, X. (2017) A review on polymeric hydrogel membranes for wound dressing applications: PVA-based hydrogel dressings. J. Adv. Res. p. 217–33. https://doi.org/10.1016/j.jare.2017.01.005

[15] Sionkowska, A. (2011) Current research on the blends of natural and synthetic polymers as new biomaterials: Review. Progress in Polymer Science, **36**, 1254–76. https://doi.org/10.1016/j.progpolymsci.2011.05.003

[16] Verbeken, D., Dierckx, S. and Dewettinck, K. (2003) Exudate gums: occurrence, production, and applications. Applied Microbiology and Biotechnology, **63**, 10–21. https://doi.org/10.1007/s00253-003-1354-z

[17] Singh, B. and Sharma, N. (2008) Development of novel hydrogels by functionalization of sterculia gum for use in anti-ulcer drug delivery. Carbohydrate Polymers, **74**, 489–97. https://doi.org/10.1016/j.carbpol.2008.04.003

[18] Singh, B., Sharma, V. and Pal, L. (2011) Formation of sterculia polysaccharide networks by gamma rays induced graft copolymerization for biomedical applications. Carbohydrate Polymers, Elsevier Ltd. **86**, 1371–80. https://doi.org/10.1016/j.carbpol.2011.06.041

[19] Singh, B. and Vashishtha, M. (2008) Development of novel hydrogels by modification of sterculia gum through radiation cross-linking polymerization for use in drug delivery. Nuclear Instruments and Methods in Physics Research Section B: Beam Interactions with Materials and Atoms, **266**, 2009–20. https://doi.org/10.1016/j.nimb.2008.03.086

[20] Singh, B. and Sharma, N. (2011) Design of sterculia gum based double potential antidiarrheal drug delivery system. Colloids and Surfaces B: Biointerfaces, Elsevier B.V. **82**, 325–32. https://doi.org/10.1016/j.colsurfb.2010.09.004

[21] Singh, B. and Sharma, N. (2009) Mechanistic implication for cross-linking in sterculia-based hydrogels and their use in GIT drug delivery. Biomacromolecules, **10**, 2515–32. https://doi.org/10.1021/bm9004645

[22] Postulkova, H., Chamradova, I., Pavlinak, D., Humpa, O., Jancar, J. and Vojtova, L. (2017) Study of effects and conditions on the solubility of natural polysaccharide gum karaya. Food Hydrocolloids, Elsevier Ltd. **67**, 148–56. https://doi.org/10.1016/j.foodhyd.2017.01.011

[23] Alves, M.-H.H., Jensen, B.E.B., Smith, A.A.A. and Zelikin, A.N. (2011) Poly(vinyl alcohol) physical hydrogels: New vista on a long serving biomaterial. Macromolecular Bioscience, **11**, 1293–313. https://doi.org/10.1002/mabi.201100145

[24] Lee, K.Y. and Mooney, D.J. (2001) Hydrogels for tissue engineering. Chemical Reviews, American Chemical Society. **101**, 1869–80. https://doi.org/10.1021/cr000108x

[25] Mansur, H.S., de, E., Mansur, A.A.P.P., Barbosa-Stancioli, E.F., de S. Costa, E., Mansur, A.A.P.P. et al. (2009) Cytocompatibility evaluation in cell-culture systems of chemically crosslinked chitosan/PVA hydrogels. Materials Science and Engineering C, **29**, 1574–83. https://doi.org/10.1016/j.msec.2008.12.012

[26] Buwalda, S.J., Boere, K.W.M., Dijkstra, P.J., Feijen, J., Vermonden, T. and Hennink, W.E. (2014) Hydrogels in a historical perspective: from simple networks to smart materials. *Journal of Controlled Release : Official Journal* of the Controlled Release Society, **190**, 254–73. https://doi.org/10.1016/j.jconrel.2014.03.052

[27] Kamoun, E.A., Chen, X., Mohy Eldin, M.S. and Kenawy, E.-R.S. (2015) Crosslinked poly(vinyl alcohol) hydrogels for wound dressing applications: A review of remarkably blended polymers. Arabian Journal of Chemistry, Elsevier. **8**, 1–14. https://doi.org/10.1016/J.ARABJC.2014.07.005

[28] Zhai, M., Yoshii, F., Kume, T. and Hashim, K. (2002) Syntheses of PVA/starch grafted hydrogels by irradiation.

Carbohydrate Polymers, **50**, 295–303. https://doi.org/10.1016/S0144-8617(02)00031-0

[29] Levi, S., Rac, V., Manojlovi, V., Raki, V., Bugarski, B., Flock, T. et al. (2011) Limonene encapsulation in alginate/poly (vinyl alcohol). Procedia Food Science, **1**, 1816–20. https://doi.org/10.1016/j.profoo.2011.09.266

[30] Kamoun, E.A., Chen, X., Mohy Eldin, M.S. and Kenawy, E.-R.S.R.S. (2014) Crosslinked poly(vinyl alcohol) hydrogels for wound dressing applications: A review of remarkably blended polymers. Arabian Journal of Chemistry, **8**, 1–14. https://doi.org/10.1016/j.arabjc.2014.07.005

[31] Hago, E. and Li, X. (2013) Based on Gelatin and PVA by Biocompatible Approaches : Synthesis and Characterization. **2013**.

[32] Razzak, M.T. and Darwis, D. (2001) Irradiation of polyvinyl alcohol and polyvinyl pyrrolidone blended hydrogel for wound dressing. Radiation Physics and Chemistry, **62**, 107–13. https://doi.org/10.1016/S0969-806X(01)00427-3

[33] Zhang, D., Chen, K., Wu, L., Wang, D. and Ge, S. (2012) Synthesis and Characterization of PVA-HA-Silk Composite Hydrogel by Orthogonal Experiment. Journal of Bionic Engineering, **9**, 234–42. https://doi.org/10.1016/S1672-6529(11)60116-9

[34] Kundu, B., Rajkhowa, R., Kundu, S.C. and Wang, X. (2013) Silk fibroin biomaterials for tissue regenerations. Advanced Drug Delivery Reviews, **65**, 457–70. https://doi.org/10.1016/j.addr.2012.09.043

[35] Wray, L.S., Hu, X., Gallego, J., Georgakoudi, I., Omenetto, F.G., Schmidt, D. et al. (2011) Effect of processing on silk-based biomaterials: Reproducibility and biocompatibility. Journal of Biomedical Materials Research - Part B Applied Biomaterials, **99 B**, 89–101. https://doi.org/10.1002/jbm.b.31875

[36] Vepari, C. and Kaplan, D.L. (2007) Silk as a Biomaterial. Progress in Polymer Science (Oxford), **32**, 991–1007. https://doi.org/10.1016/j.progpolymsci.2007.05.013

[37] Altman, G.H., Diaz, F., Jakuba, C., Calabro, T., Horan, R.L., Chen, J. et al. (2003) Silk-based biomaterials. Biomaterials, **24**, 401–16. https://doi.org/10.1016/S0142-9612(02)00353-8

[38] Lu, S., Wang, X., Lu, Q., Zhang, X., Kluge, J.A., Uppal, N. et al. (2010) Insoluble and flexible silk films containing glycerol. Biomacromolecules, **11**, 143–50. https://doi.org/10.1021/bm900993n

[39] Ziv, K., Nuhn, H., Ben-Haim, Y., Sasportas, L.S., Kempen, P.J., Niedringhaus, T.P. et al. (2014) A tunable silk-alginate hydrogel scaffold for stem cell culture and transplantation. Biomaterials, **35**, 3736–43. https://doi.org/10.1016/j.biomaterials.2014.01.029

[40] Hu, X., Lu, Q., Sun, L., Cebe, P., Wang, X., Zhang, X. et al. (2010) Biomaterials from ultrasonication-induced silk fibroin-hyaluronic acid hydrogels. Biomacromolecules, **11**, 3178–88. https://doi.org/10.1021/bm1010504

[41] Silva, S.S., Santos, T.C., Cerqueira, M.T., Marques, A.P., Reys, L.L., Silva, T.H. et al. (2012) The use of ionic liquids in the processing of chitosan/silk hydrogels for biomedical applications. Green Chemistry, **14**, 1463. https://doi.org/10.1039/c2gc16535j

[42] Tsukada, M., Freddi, G. and Crichton, J.S. (1994) Structure and Compatibility of Poly (vinyl Alcohol) -Silk Fibroin (PVA / SF) Blend Films. Journal of Polymer Science; Polymer Physics, **32**, 243–8.

[43] Li, J.H., Cao, C.B., Ma, X., Tang, Y. and Zhu, H.S. (2005) The antithrombogenecity of silk fibroin films blending with citric acid and PVA. Key Engineering Materials, **288**–**289**, 417–20.

[44] Kundu, J., Poole-Warren, L.A., Martens, P. and Kundu, S.C. (2012) Silk fibroin/poly(vinyl alcohol) photocrosslinked hydrogels for delivery of macromolecular drugs. Acta Biomaterialia, **8**, 1720–9. https://doi.org/10.1016/j.actbio.2012.01.004

[45] Wang, X., Partlow, B., Liu, J., Zheng, Z., Su, B., Wang, Y. et al. (2015) Injectable silk-polyethylene glycol hydrogels. Acta Biomaterialia, **12**, 51–61. https://doi.org/10.1016/j.actbio.2014.10.027

[46] Mandal, B.B., Kapoor, S. and Kundu, S.C. (2009) Silk fibroin/polyacrylamide semi-interpenetrating network hydrogels for??controlled drug release. Biomaterials, **30**, 2826–36. https://doi.org/10.1016/j.biomaterials.2009.01.040

[47] Chen, G., Liu, C., Zhang, B., Xu, G. and Huang, Y. (2014) Swelling behaviours of silk fibroin-polyurethane composite hydrogels. Asian Journal of Chemistry, **26**, 1533–6. https://doi.org/10.14233/ajchem.2014.17280

[48] Dai, L., Li, J. and Yamada, E. (2002) Effect of glycerin on structure transition of PVA/SF blends. Journal of Applied Polymer Science, **86**, 2342–7. https://doi.org/10.1002/app.11260

[49] Lee, J.W., Ashby, R.D. and Day, D.F. (1996) Role of acetylation on metal induced precipitation of alginates. Carbohydrate Polymers, **29**, 337–45. https://doi.org/10.1016/S0144-8617(96)00017-3

[50] Singh, B., Sharma, V. and Chauhan, D. (2010) Gastroretentive floating sterculia–alginate beads for use in antiulcer drug delivery. Chemical Engineering Research and Design, **88**, 997–1012. https://doi.org/10.1016/j.cherd.2010.01.017

[51] Yuen, S.-N., Choi, S.-M., Phillips, D.L. and Ma, C.-Y. (2009) Raman and FTIR spectroscopic study of carboxymethylated non-starch polysaccharides. Food Chemistry, **114**, 1091–8. https://doi.org/10.1016/j.foodchem.2008.10.053

[52] Mansur, H.S., Sadahira, C.M., Souza, A.N. and Mansur, A.A.P. (2008) FTIR spectroscopy characterization of poly (vinyl alcohol) hydrogel with different hydrolysis degree and chemically crosslinked with glutaraldehyde. Materials Science and Engineering: C, **28**, 539–48. https://doi.org/10.1016/j.msec.2007.10.088

[53] Zhao, L., Mitomo, H., Zhai, M., Yoshii, F., Nagasawa, N. and Kume, T. (2003) Synthesis of antibacterial PVA/CM-chitosan blend hydrogels with electron beam irradiation. Carbohydrate Polymers, **53**, 439–46. https://doi.org/10.1016/S0144-8617(03)00103-6

[54] Laity, P.R., Gilks, S.E. and Holland, C. (2015) Rheological behaviour of native silk feedstocks. Polymer, **67**, 28–39. https://doi.org/10.1016/j.polymer.2015.04.049

[55] Sionkowska, A. and Planecka, A. (2011) The influence of UV radiation on silk fibroin. Polymer Degradation and Stability, **96**, 523–8. https://doi.org/10.1016/j.polymdegradstab.2011.01.001

[56] THOMAS, O. and BURGESS, C. (2007) UV-visible spectrophotometry of water and wastewater. Elsevier, Boston.

[57] Wang, X., Yucel, T., Lu, Q., Hu, X. and Kaplan, D.L. (2010) Silk nanospheres and microspheres from silk/pva blend films for drug delivery. Biomaterials, **31**, 1025–35.

https://doi.org/10.1016/j.biomaterials.2009.11.002

[58] Koebley, S.R., Thorpe, D., Pang, P., Chrisochoides, P., Greving, I., Vollrath, F. et al. (2015) Silk reconstitution disrupts fibroin self-assembly. Biomacromolecules, **16**, 2796–804. https://doi.org/10.1021/acs.biomac.5b00732

[59] Jessie Lue, S., Chen, J. and Ming Yang, J. Crystallinity and Stability of Poly(vinyl alcohol)- Fumed Silica Mixed Matrix Membranes. https://doi.org/10.1080/15568310701744133

[60] Lu, S., Wang, X., Lu, Q., Zhang, X., Kluge, J.A., Uppal, N. et al. (2010) Insoluble and Flexible Silk Films Containing Glycerol. Biomacromolecules, American Chemical Society. **11**, 143–50. https://doi.org/10.1021/bm900993n

[61] Guan, J., Wang, Y., Mortimer, B., Holland, C., Shao, Z., Porter, D. et al. (2016) Glass transitions in native silk fibres studied by dynamic mechanical thermal analysis. Soft Matter, **12**, 5926–36. https://doi.org/10.1039/c6sm00019c

[62] Neo, P.Y., Shi, P., Goh, J.C.-H. and Toh, S.L. (2014) Characterization and mechanical performance study of silk/PVA cryogels: towards nucleus pulposus tissue engineering. Biomedical Materials, **9**, 065002. https://doi.org/10.1088/1748-6041/9/6/065002

[63] Assender, H.E. and Windle, A.H. (1998) Crystallinity in poly(vinyl alcohol). 1. An X-ray diffraction study of atactic PVOH. Polymer, **39**, 4295–302. https://doi.org/10.1016/S0032-3861(97)10296-8

[64] Zhang, X., Reagan, M.R. and Kaplan, D.L. (2009) Electrospun silk biomaterial scaffolds for regenerative medicine. Advanced Drug Delivery Reviews, Elsevier. **61**, 988–1006. https://doi.org/10.1016/J.ADDR.2009.07.005

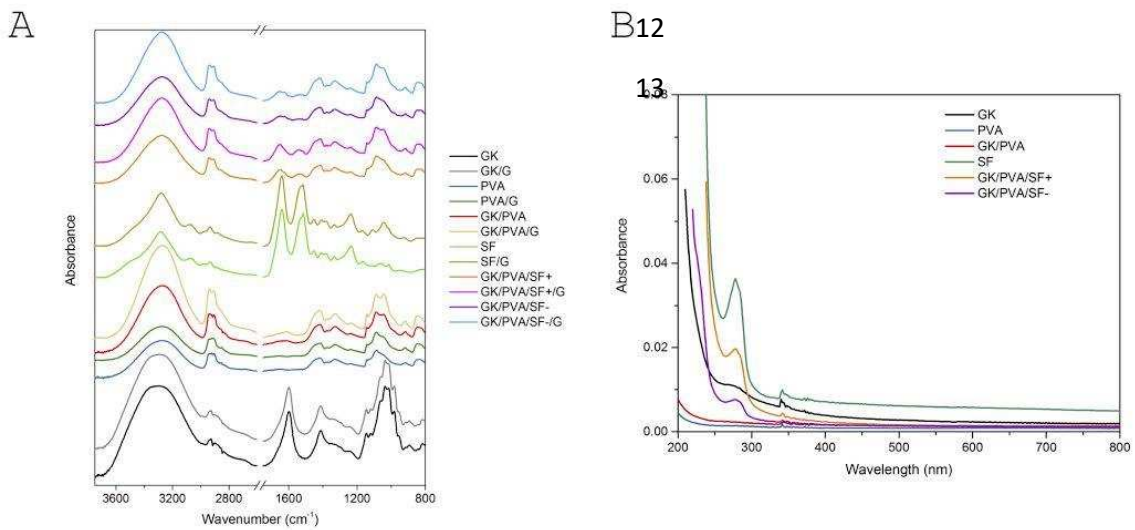

Figure 1: A) FTIR ATR spectra of prepared xerogel films (GK = gum karaya, PVA = poly(vinyl alcohol), SF = silk fibroin, G = glycerol, + represents higher silk ratio, - represents lower silk ratio), B) UV/VIS spectra of prepared xerogel films with the small amount of noise at 340 nm being caused by the deuterium to halogen lamp change.

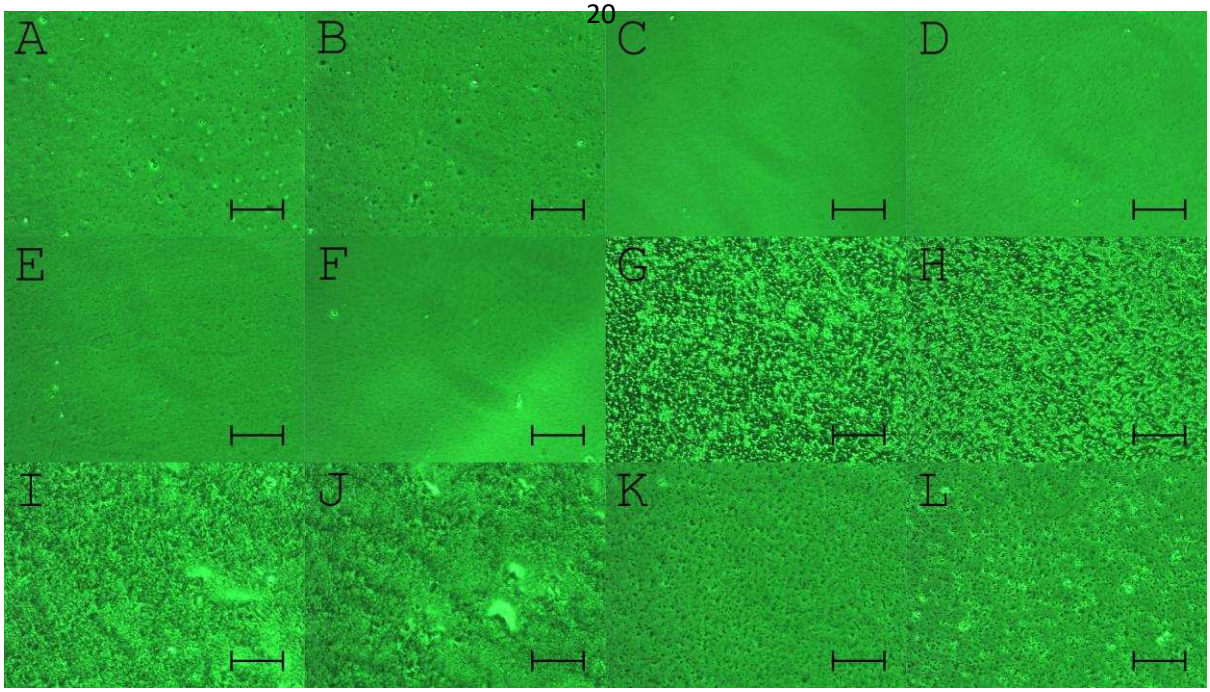

Figure 2: Phase contrast microscopy pictures of prepared xerogel films: A) GK, B) GK/G, C) PVA, D) PVA/G, E) GK/PVA, F) GK/PVA/G, G) SF, H) SF/G, I) GK/PVA/SF+, J) GK/PVA/SF+/G, K) GK/PVA/SF- and L) GK/PVA/SF-/G (scale bar for all pictures is 100 µm).

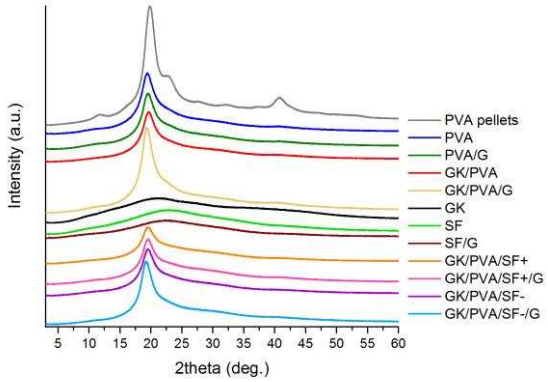

Figure 3: XRD spectra of PVA pellets, PVA, GK/PVA, SF, GK/PVA/SF+, GK/PVA/SF+/G, GK/PVA/SF- and GK/PVA/SF-/G (samples tested in xerogel film form apart from PVA pellets).

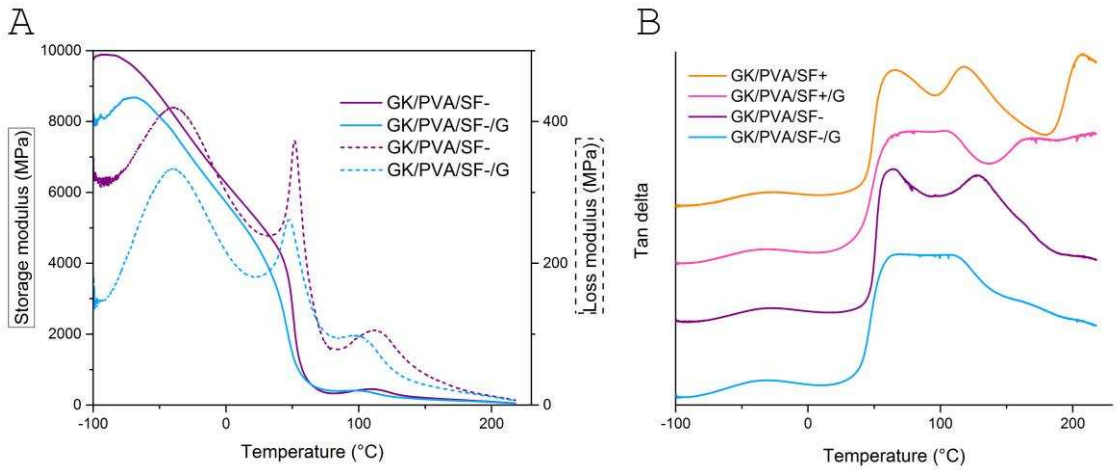

Figure 4: A) Storage and loss modulus for samples and GK/PVA/SF-/G, B) Tan delta for samples GK/PVA/SF+, GK/PVA/SF+/G, GK/PVA/SF- and GK/PVA/SF-/G.

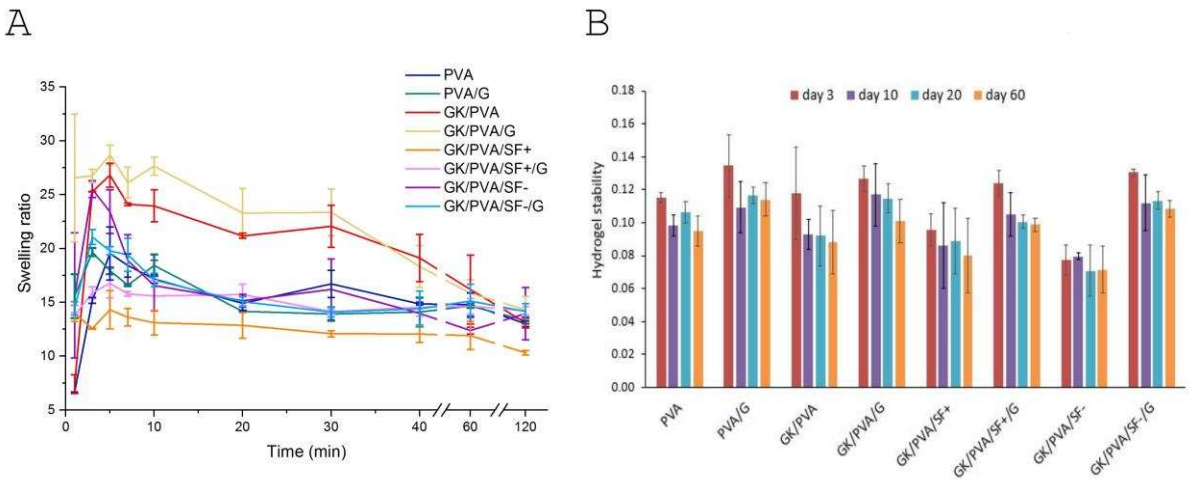

Figure 5: A) Swelling ratio of prepared hydrogels depending on time, B) Hydrogel stability on day 3, 10, 20 and 60 (Type I water at 37°C).

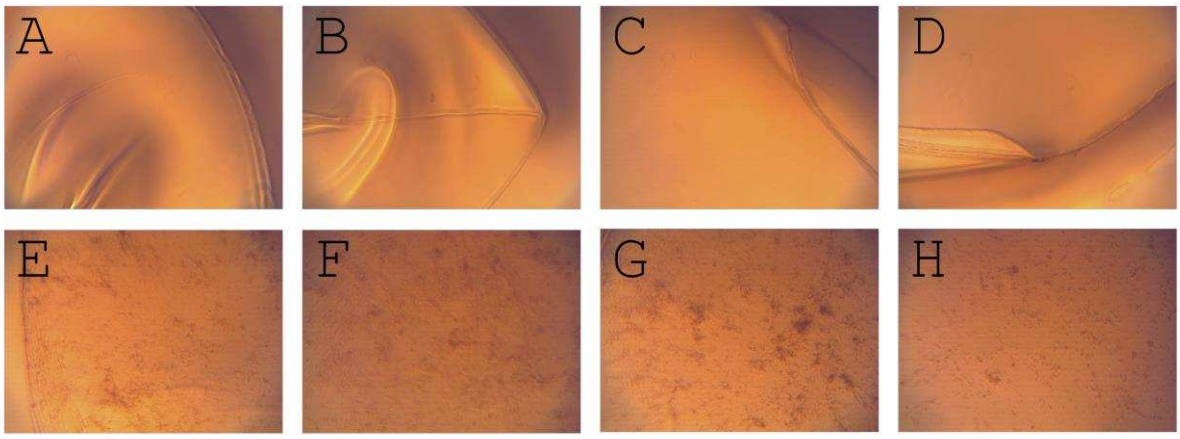

Figure 6: Microscope picture of hydrogel surfaces after adhesion assay: A) PVA, B) PVA/G, C) GK/PVA, D) GK/PVA/G, E) GK/PVA/SF+, F) GK/PVA/SF+/G, G) GK/PVA/SF-, H) GK/PVA/SF-/G (magnification 7.5).

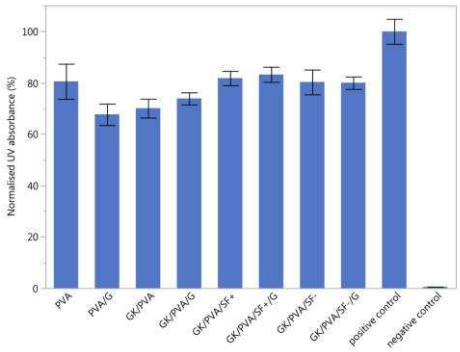

Figure 7: MTT assay: Normalised UV absorbance corresponding to activity of keratinocytes layer on TCP after hydrogel removal.